DEVELOPMENT OF A VALIDATED THERMAL MODEL OF AC PERFORMANCE IN A PROTECTED COMBAT GROUND VEHICLE

Josh Pryor
Aaron Ditty
Julia Mao
Pete Rynes
ThermoAnalytics, Inc.

Rob Smith
TARDEC
Warren, MI

ABSTRACT

A coupled thermal and computational fluid dynamics (CFD) full-vehicle model of a protected combat ground vehicle was developed and validated against measured test data. The measurement dataset was collected under thermally extreme conditions. Air temperatures were sampled inside the crew compartment of the vehicle under tactical idle operating conditions with space heaters substituted for on-board electronics. The results generated from the coupled thermal model correlated with the measured test data with an average absolute error of less than 2 °F for both simulated-electronics on and off conditions. The model was used to analyze thermal sensitivity to armor, insulation, and other factors affecting the efficiency of the HVAC system.

OBJECTIVE

The objective of this work is to develop a full vehicle thermal simulation of a ground vehicle, and to validate the thermal model using measured test cell data. Validation tests were run in a test cell under tactical idle conditions, with the AC system active and space heaters representing electronic thermal loading. Air temperatures, measured inside the vehicle by the vehicle integrator, serve as the validation data set. The desired outcome is a quantifiable assessment of the accuracy of the ground vehicle thermal model under the specified test cell conditions, which would allow the thermal model to be used to predict vehicle thermal performance under expected battlefield conditions.

BACKGROUND

Previous full-vehicle simulations had been performed using this ground vehicle model to quantify thermal management issues caused by including additional electronics into the vehicle cabin. In these studies, the vehicle was simulated at 20 MPH using worst-case boundary conditions, for both open and closed hatch scenarios.

To validate this vehicle thermal model, simulations were conducted of the vehicle operated inside a test cell. Conditions within the test cell differed from those used in the previous simulations. During the tests, the vehicle was exposed to a 5 MPH wind with an ambient air temperature of 130 °F and an 1120 W/m^2 solar load. The validation data consisted primarily of interior air temperatures at 18 locations representing the head, chest, and feet locations for 6 occupants inside the cabin. Unfortunately, no test data was available on the powertrain performance or on its heat rejection. Also, no surface temperature measurements were made during the test; such data would have been valuable in defining the thermal loads imposed by the powertrain on the vehicle body and in assessing the root causes of observed differences between the test data and the simulation results. In the test cell, a light bank provided artificial solar loading, however, the bulbs used in the light bank were not solar simulators but heat lamps, which have different spectral properties than the sun. The light bank, consequentially, required special handling in the simulation.

SUMMARY

Thermal and computational fluid dynamics (CFD) simulations were created for the ground vehicle. The simulation included external (under-hood/under-body) and interior (cabin) CFD models to accurately predict localized flow and convection coefficients. The MuSES (Multi-Service Electro-optic Signature) thermal simulation was used to capture the effects of the environmental loads and accurately predict surface temperatures accounting for all modes of heat transfer. The thermal and CFD solutions were coupled for a complete thermal solution.

The wind, air temperature, and solar load conditions within the test cell were modeled within the simulations. The engine and cooling system were simulated in a tactical idle condition. The air conditioning (AC) system flow rates and cooling capacity were provided from test data and vendor information. The heat load inside the cabin was determined from the space heater specifications. Vehicle insulation properties were provided by the vehicle manufacturer.

MEASUREMENT DATA

The measurement data for the thermal test was provided by the vehicle integrator. A vehicle without electronics, human/manikins, or GPK (Gunner Protection Kit) was tested with the AC on and two heaters representing the electronic heat load. Humans would have added to the heat load and would have impacted the interior air flow, while the GPK would have affected the exterior air flow. The hatch was

closed and the ambient temperature was 130 °F. Prior to the transient temperature data shown in Figure 1, conditions within the test cell and the vehicle, with all systems off, were allowed to equilibrate. At this point in the test, at 1:48 PM in Figure 1, the engine was set to tactical idle and the AC engaged. Once air temperatures inside the vehicle cooled down and stabilized, the heaters representing the electronics heat load were turned on; by 6:15 PM temperatures inside the vehicle had once again stabilized.

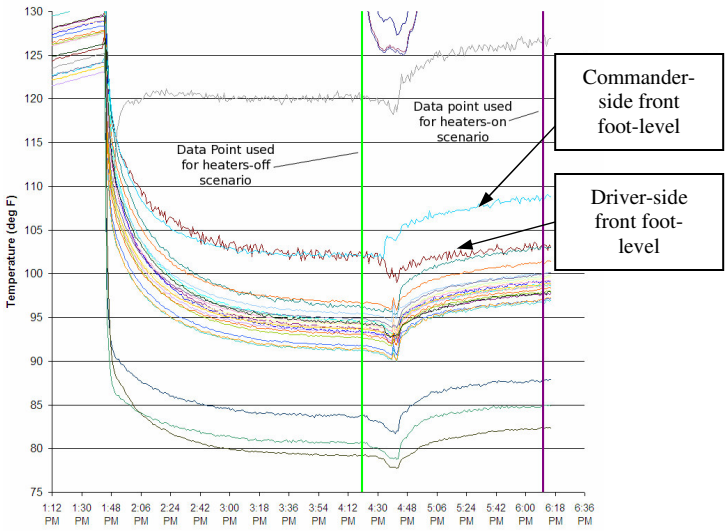

Figure 1: Sample of Transient Measurement Data

Several trends are noteworthy within this data. During the transition between the heaters-off and heaters-on segments of the test, there is a dip in nearly all the data points that is unexplained by the testing procedure. Additionally, the data taken at this time (around 4:45 PM) for the driver-side foot position, shown in red-brown in Figure 1 between 100 and 105 °F, shows a temperature drop of only 1.2 F and the data for the commander foot position, shown in light blue between 100 and 110 °F, shows a temperature rise whereas all other locations show a temperature dip of between 4 and 7 F. There is no explanation in the test procedure for these data inconsistencies.

MODEL DESCRIPTION

Geometry

The geometry cleanup and meshing were performed using ANSA® software from Beta CAE. MuSES is a shell based solver, therefore we needed to convert all 3D parts to a surface description. To reduce the 3D part geometry to a surface description, we created a 2D surface through the mid plane of the 3D geometry and assigned the correct thickness to the MuSES part. Bolts, fasteners, small holes and gaps were eliminated to achieve a high quality thermal mesh. We produced three separate mesh models for this work: a thermal mesh for MuSES, and interior and exterior flow meshes for Fluent CFD. In the thermal model, geometry for the environmental chamber was included to capture the effect of solar and thermal radiation from the light bank. The final mesh counts were approximately 200,000 surface elements for the MuSES thermal model, 11 million volume elements for the internal CFD model, and 21 million elements for the external CFD model.

Figure 2 shows the process by which the MuSES thermal model was coupled to the two (interior and exterior) CFD models. At the conclusion of each CFD iteration, MuSES exchanged information with Fluent: MuSES passed wall temperatures to Fluent, which in turn passed convection coefficients and film temperatures for all interior and exterior vehicle surfaces back to MuSES. Since MuSES iterates an order of magnitude faster than Fluent this resulted in the data exchange occurring after every 10 to 20 MuSES iterations. These coupled iterations continued until the calculated temperatures converged in both thermal and CFD.

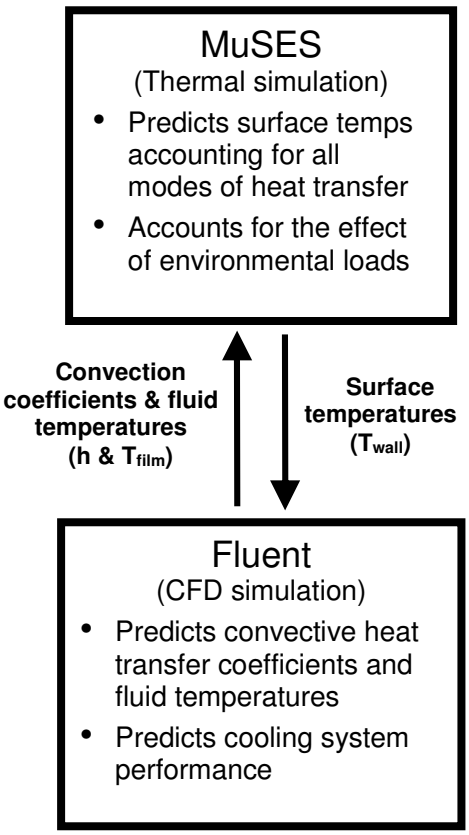

Figure 2: MuSES/CFD Coupling Process

Thermal Boundary Conditions

Thermal boundary conditions were set on the meshed vehicle geometry using MuSES Pro 9.2.0. Thicknesses were extracted from the 3D solid geometry, and, for parts representing layered armor and for parts separated by an air gap, thin shell layers were created and thermally linked using face to face conduction. We chose to model these layered parts using separate parts rather than an N-Layer part so that we could preserve the correct positioning of the front and back surfaces for the CFD analysis. All exterior parts were assigned the solar absorptance and thermal emissivity of CARC tan paint. Convective heat transfer boundary conditions assigned to the vehicle surfaces came from the coupling with CFD. The layered thermal insulation for the interior of the cabin was modeled per information provided by the vehicle manufacturer.

Environmental Modeling

The environmental chamber geometry was explicitly modeled in MuSES. The cylindrical chamber geometry completely surrounded and enclosed the vehicle except for a rectangular cut-out in the chamber ceiling. We positioned the cut-out and the sun to represent the light bank. Using the MuSES sun model, a parallel beam of solar radiation passed through the 'light bank' cut-out and was incident on the vehicle and the chamber interior. This method accurately modeled solar reflections off the chamber floor and walls. The surface emissivity of the chamber walls were measured on-site and the wall temperatures were provided by test-site engineers.

The solar absorptance of the CARC tan paint on the vehicle required modification due to differences in the radiation spectrum between the heat lamps used in the test cell light bank and the natural sun. Two pyranometers on the vehicle roof measured the heat flux from these lamps to be 1120 W/m^2. The spectrum emitted from these lamps, which have a filament temperature of around 2800 K, is shifted more towards the near infrared than that of the sun, which has an apparent temperature of ~5800 K. Based on these different spectrums, including the spectral transmission through the bulb glass and the atmosphere, we adjusted the solar absorptance of the CARC tan paint from 0.48 to 0.411. This effectively reduced the solar load to 955 W/m^2.

We also accounted for the thermal radiation from the light bank to the vehicle. We calculated an approximate average temperature for the light bank and bulbs (136 °F) and assigned this temperature to the sky in the MuSES weather file. Using the MuSES natural environment model, the light produced by the light bank was modeled using the natural sun while the thermal radiation of the light bank was modeled using the sky radiation model; the cut-out in the chamber ceiling allowed both the light and the thermal sky radiation to enter the model of test chamber.

Powertrain Modeling

The engine and transmission are modeled as fixed-temperature parts, at 95 °C and 80 °C respectively. The exhaust is modeled using a fluid stream, with an upstream temperature of 300 °C in the manifold. The fluid stream model computes the gas temperature throughout the length of the exhaust pipe as it loses heat through the pipe walls.

CFD Model Setup

We used Fluent® 6.3 from ANSYS to solve for both the external and internal air flows. For both volume meshes, the air flow is assumed to be compressible and turbulent. Turbulence is modeled using the standard k-epsilon turbulence model and standard wall functions at the walls. Compressibility and buoyancy are modeled using the incompressible ideal gas equation of state (density as a function of temperature). The solution is obtained using the pressure-based segregated algorithm.

External CFD Boundary Conditions

The boundary conditions for the external case are shown in Table 1. To properly simulate under hood temperatures, the effect of heat exchangers must be modeled. The targeted fan flow rate was based on previous work with a vehicle that had a similar engine fan. Since detailed heat exchange information was not available, we used a simple model for the cooling pack; the applied heat load of 20 kW was based on input from the engine manufacturer.

Table 1: External CFD Boundary Conditions

Boundary	Boundary Condition
Bounding box (inlet)	Velocity = Vehicle speed of 5 MPH Temperature = 54 °C (327.6 K) Turbulent intensity = 5% with length scale = 0.5 m
Bounding box (outlet & walls)	Pressure = 0 (gauge)
Vehicle surfaces	Velocity = 0 (no-slip) for non-moving surfaces; wheels and tires given rotational velocity Temperature coupled w/MuSES
Tailpipe outlet	Mass flow = 0.1 kg/s Temperature coupled w/MuSES Turbulent intensity=15% with length scale=20 mm
Engine intake inlet	Mass flow = -0.1 kg/s
Engine fan	Pressure jump targeted to achieve ~7 kg/s airflow

Internal (Cabin) CFD Boundary Conditions

As in the external case, the wall surfaces of the interior CFD simulation were modeled as non-slip walls with their temperatures coupled with MuSES. The vehicle contained two AC systems, one in the front and one in the rear. We modeled both AC systems in recirculation mode with no

ingestion of fresh air. We did not have sufficient geometry and data to model components within the HVAC system, such as the blower and evaporator core. This required a boundary condition of a flow rate and temperature at the inlet to the ductwork. We set the temperatures based on test measurements, and the flow rates on guidance from the vehicle manufacturer. We included geometric details of the ductwork for the rear AC system into the simulation so that the CFD could compute the distribution of the flow to the various vents. Since the vents for the front AC are within close proximity, we assumed that the flow rate was equal for all vents. The system return was modeled as a pressure outlet in order to conserve mass in the system.

RESULTS

Simplified Test Model

A reduced MuSES model was used to test changes to the full validation model and determine their approximate impact. This model utilizes a smaller subset of the vehicle geometry and only predicts the bulk air temperature inside the cabin. The purpose of this model was to quickly investigate single changes as more information is discovered about the vehicle and test scenario and determine their relative impact on the results. Trying each of these changes individually on the full coupled thermal model would have been impractical due to runtime. Additionally, applying all discovered changes to the model does not give an understanding of which changes are most important to the results.

Table 2 shows the results from the simplified test model. It should be noted that these relative magnitudes are representative of this specific vehicle only – much of the information that determines these changes varies with vehicle, such as armor configuration, insulation properties, powertrain layout, and others.

Model Changes	Approx. ΔTemp	Details
Inclusion of insulation inside cabin	**-12 ˚F**	Updated material properties. Added insulation in the tunnel, firewall and floor, compared to no insulation in these areas
Inclusion of surround chamber geometry	**-8 ˚F**	Added chamber geometry and correct measured surface conditions, compared to geometry-less environment
Increases AC Flow rates	**-7 ˚F**	Increased air mass flow by approximately 33% with constant vent temperature
Decreased cooling pack heat rejection and exhaust T	**-5 ˚F**	Reduced heat load by approximately 80 kW and decreased exhaust temperature by 300 °C
Update to paint absorptance due to the effects of lamps vs. solar	**-1 ˚F**	Reduced paint absorptance based on spectral emission differences between test cell heat lamp array and the sun
Heater adjustments	**+2 ˚F**	Decreases heater surface T and increased heater air temperature to better represent realistic physical performance.

Table 2: Results from Simplified Validation Model

Full Vehicle Validation Models

Figure 3 shows a comparison between measured test data and the results from the initial baseline simulation after updating the model as described above. After this comparison was made, we received additional data from the engine and vehicle manufacturer that allowed us to improve the modeling of the powertrain.

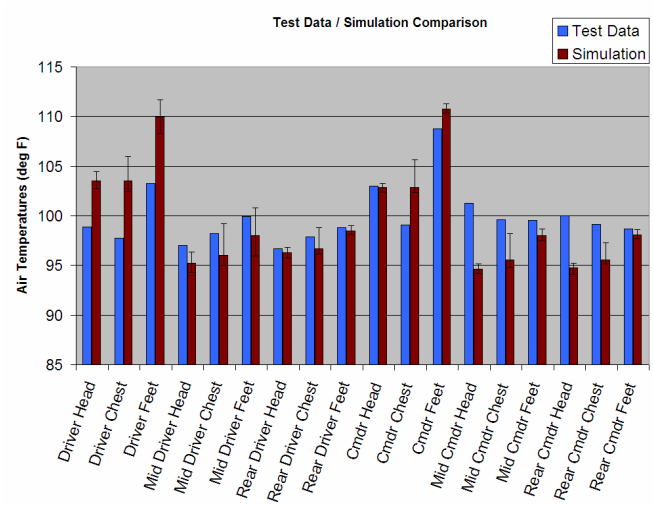

Average absolute error	Front cabin average error	Rear cabin average error
2.9 F	+3.8 F	-2.5 F

Figure 3: Test Data Comparison, Baseline Simulation

During the test, no data was taken on the engine speed, output, heat rejection, or exhaust temperatures. Based on a description of the known test conditions, the engine manufacturer provided an estimate of the two main engine parameters needed for this model: exhaust manifold temperature and cooling pack heat rejection.

We also updated the modeling of the ceramic heaters based on manufacturer information; this resulted in more realistic modeling of surface and air temperatures. We also updated the AC vent temperatures based on test data; we could not use this data directly since the test measurements were made at the AC registers whereas the model required boundary conditions at the ductwork inlet.

Figure 4 shows the measurement-model temperature comparison after we had made these changes to the thermal and CFD models. The main effect of the changes was a reduction in error in the front of the vehicle due to less underbody heat loading. The change in the heater air temperature and vent temperatures also slightly improved the results in the rear of the cabin.

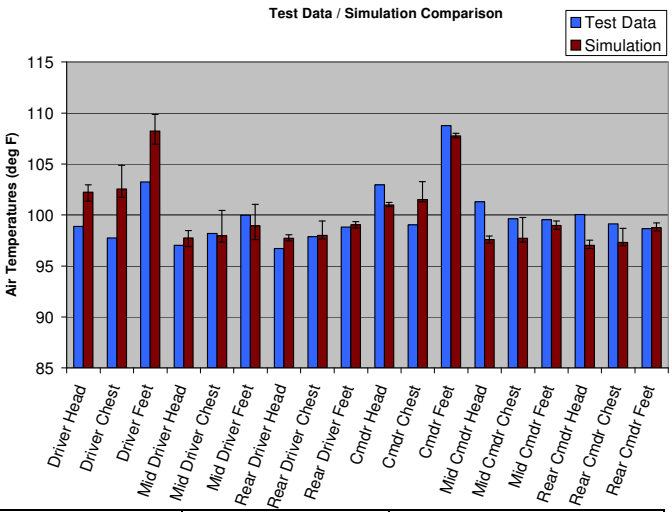

Average absolute error	Front cabin average error	Rear cabin average error
1.8 F	+2.1 F	-0.8 F

Figure 4: Test Data Comparison w/Powertrain Updates

The simulation results shown in Figure 4 are, in general, a close match to the measured data, given the lack of detail about some of the vehicle components and test conditions, the desired output of this model, and the variability in the test data. Two significant differences seem to stand out: an over-prediction of temperatures for all three driver measurements, and a reversal in temperature trends from head to feet in both the mid and rear commander side measurements. Both of these discrepancies will be discussed below.

Full-Vehicle Model (Heaters-Off Scenario)

As previously discussed, Figure 1 shows some inconsistent behavior in the rise in temperature on the driver's measurements after the space heaters inside the cab are activated. Since no explanation was apparent from the test data as to the cause of this behavior, a heaters-off scenario was simulated in order to further evaluate the effectiveness of the model.

For this model, all boundary conditions and setup remain the same except for the removal of the 3kW of heat imposed by the space heaters. Figure 5 shows the comparison between this model and the measured data.

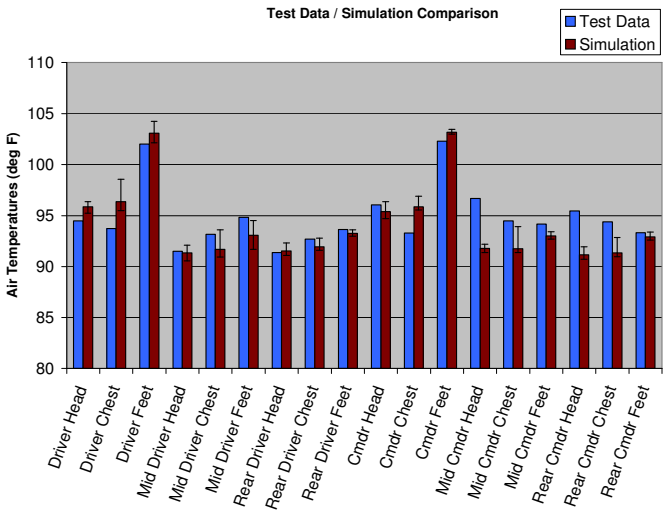

Average absolute error	Front cabin average error	Rear cabin average error
1.7 F	+1.3 F	-1.7 F

Figure 5: Test Data Comparison, Heaters-Off Scenario

Compared to the heaters-on scenario, there is a significant improvement in the driver's area. This result confirms that some inconsistent behavior occured in the driver's area when the heaters are turned on (the rise in temperature is smaller than the rest of the cabin.) This phenomenon can be further demonstrated by comparing the change in temperature at all 18 locations between the heater-off and heater-on condition, as shown in Figure 6.

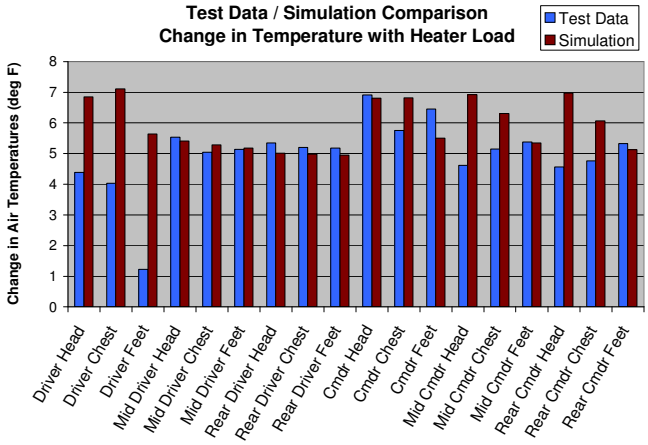

Figure 6: Comparison of Temperature Change caused by Heaters, Test Data and Simulation

This shows that the rise in temperature induced by the heaters was fairly consistent in the majority of locations, typically between 5 and 7 °F. The test data for the driver, however, did not follow this trend as they increased by only 1 to 4 °F. The simulation did not model this deviation from the trend; the simulation showed a rise in temperature that was consistent throughout the vehicle cabin.

This comparison is also useful since the original goal of this model was to predict the thermal behavior of the vehicle when electronic heat loads are added inside the cabin. Based on the similar results of the test and simulation, the model is an appropriate tool for predicting this sort of behavior.

Investigation of Vent Direction

As seen in previous test data comparisons, the test data showed higher temperatures towards the head, and lower temperatures towards the feet, for both of the rear occupants on the commander side. Simulations consistently showed the opposite gradient. The behavior seen in the simulation was expected since the AC air vents are located along the ceiling of the cabin and most heat sources, such as the powertrain, are directed toward the floor of the cabin.

One possible explanation for this behavior is vent position. The test procedure involved pointing all vents straight out, but some field reports suggest that the angle of the vents shifted when the AC blower was turned on. To examine the hypothesis that the vents may have been shifted during the test, we decided to run a simulation with the vents on the commander side of the rear AC system pointing down at approximately 45° to direct the cool air away from head level of the occupants. Figure 7 shows some of the results from this simulation.

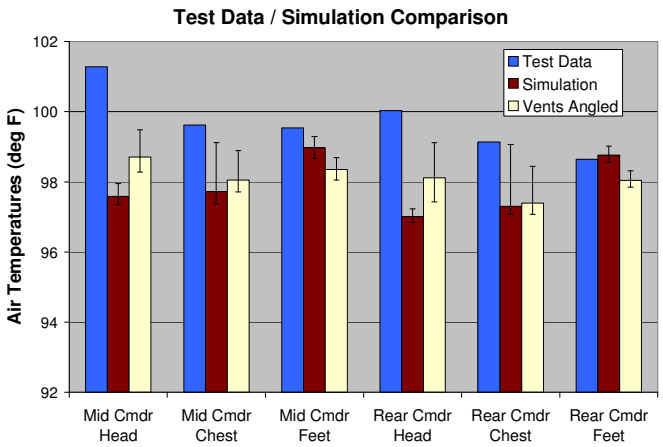

Figure 7: Comparison of Test Data, Simulation w/ Baseline Vents, and Simulation w/ Vents Angled

Redirecting the rear AC vents caused some reversal of the temperature gradient from head to feet, but there is still some

discrepancy between the simulation and the test data. This change also caused undesired behavior in other locations in the cabin, so this change was not used for the final validation model. This investigation does, however, demonstrate that vent position may be partly responsible for the inconsistencies noted in the test data for the rear cabin.

CONCLUSIONS/RECOMMENDATIONS

The level of agreement between the final validation model and the measured test data, as illustrate by Figure , indicates that the thermal model has sufficient fidelity and accuracy for thermal analysis and trade studies. The agreement is not perfect, but the model-to-test comparison is restricted by the lack of some crucial pieces of testing data and vehicle component details. Given the variability and unknown quantities present in the test, a closer level of agreement cannot be expected.

This validation effort demonstrates that a full-vehicle thermal simulation can be a valuable tool for evaluating thermal performance of the ground vehicle when relevant boundary conditions are known. The validation shows that this model can be used to predict the thermal performance of the vehicle when high-powered electronics is added inside the cabin.

Future work may include both validating the model against a test done with actual electronics inside the cabin, as well as modeling the required AC capacity to maintain required temperature levels given heavy electronic thermal loads.

ACKNOWLEDGEMENTS

TAI would like to acknowledge the following individuals for their critical support during this validation effort.

- TARDEC
  - Rob Smith (CASSI)
  - Andrew Schultz